Figure 4 demonstrates the effect of f_{O_2} on the σ of olivine from the Red Sea area [15] as a function of temperature to 1500 °C. As can be seen from Fig. 2, our gas mixer does not allow close approach to oxidation, but allows for reduction, of olivine. Data presented in Fig. 4 were obtained within the stability field of olivine and show a dependence that is approximately pro-

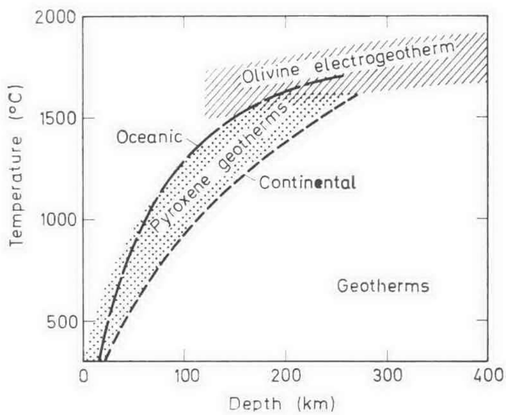

Fig. 5. The temperature vs. depth profile calculated from line 6a in Fig. 3, and the σ vs. depth data discussed in the text. The pyroxene geotherms (BOYD [3]; MACGREGOR and BASU [25]; and MERCIER and CARTER [27]) and postulated continental and oceanic geotherms (RINGWOOD [36]) are shown for comparison

portional to $(f_{O_2})^{+1/6}$ at high f_{O_2} but approximately proportional to $(f_{O_2})^{-1/12}$ at low f_{O_2}. From the work of SMYTH and STOCKER [42], this is consistent with a mechanism dependent on oxidation of ferrous to ferric iron at high f_{O_2} but the slope at low f_{O_2} does not fit a simple oxygen defect model. A similar interpretation for high f_{O_2} was made by SHANKLAND [41] for results which were obtained by PARKIN [32] for σ measured on Fe-doped synthetic forsterite under controlled f_{O_2}. The results of DUBA et al. [15], at low f_{O_2} are not consistent with SHANKLAND's interpretation of PARKIN's data for low f_{O_2}.

Figure 5 shows the geotherm calculated from line 6b of Fig. 3 and literature data for σ of the earth's mantle between 100 and 400 km [37, 22, 2, 30, 43]. The broad span in temperature is due to the range of σ values reported by these authors. The use of line 6b is reasonable if olivine of composition Fo 90 controls the σ of the earth's mantle since the σ of olivines of similar compositions and quite different histories (lines 6b and 7b, Fig. 3) agree very well under controlled f_{O_2}. Also shown in Fig. 5 are the limits of various values reported for geotherms calculated from pyroxene inclusions in nodules derived from the upper mantle [3, 27, 25] and the continental and oceanic geotherms proposed by RINGWOOD [36]. From this figure it is clear that a mantle whose σ is controlled by olivine is consistent with a reasonable geotherm at depths greater than about 150 km. At shallower depths, however, the temperatures are considerably higher than expected. This suggests σ is controlled in the outer 150 km by other more conducting phases, perhaps interstitial water, partial melts, and other grain boundary impurities, or some other mineral species.

3. The effect of order—disorder and partial melt on σ

Khitarov and Slutskii [23] have shown that the σ of albite, the Na-rich end-member of the plagioclase feldspar series, increases three to four orders of magnitude upon melting (solid and dashed lines, Fig. 6). Piwinskii and Duba [33], however, have shown that the σ of albite increases a similar

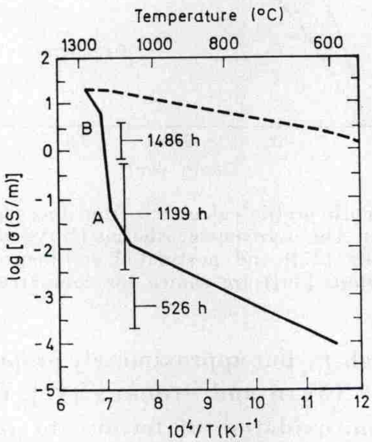

Fig. 6. The electrical conductivity of albite. Solid line is for polycrystalline albite prior to melting; dashed line is same sample during and after melting (Khitarov and Slutskii [23]). The vertical lines are measured as a function of time as indicated at temperature below the solidus (Piwinskii and Duba [33])

amount below melting provided time is allowed for disorder to proceed. These data are shown as the solid vertical lines in Fig. 6.

More recent work [15] on basalt containing about 35% plagioclase indicates that σ increases with time subsolidus. These data are shown in Fig. 7 in which a comparison is made among the σ of samples from the same rock at various f_{O_2} and with differing time-temperature histories. The figure clearly demonstrates that the σ change upon partial fusion at 1050 °C (solidus temperature is 1020 ± 8 °C) is dependent on the time spent near but below the beginning of melting by the sample. The σ is also dependent on f_{O_2} in this rock. Studies such as those of Presnall et al. [35] and Watanabe [44] and Khitarov and Slutskii [23] on basalt and that of Lebedev and Khita-